Physical Modelling in Geotechnics – Gaudin & White (Eds)
© 2014 Taylor & Francis Group, London, ISBN 978-1-138-00152-7

Seismic behavior of inverted T-shape flexible retaining walls via dynamic centrifuge

S.B. Jo, J.G. Ha, M.T. Yoo, Y.W. Choo & D.S. Kim
KAIST (Korea Advanced Institute of Science and Technology), Daejeon, Republic of Korea

ABSTRACT: The behavior of inverted T-shape flexible retaining walls under seismic loadings was experimentally investigated. Two centrifuge tests were carried out on reduced-scale models of flexible retaining walls with different heights in dry sand. The experimental data showed that acceleration amplification is not affected by the wall height. The acceleration of the backfill was not uniform and a phase difference was measured between the wall and backfill soil. During the maximum bending moments of the wall, dynamic earth pressures were only measured at the bottom area of the wall. The inertial force of the wall induced deflection of the wall to result in gapping between the wall and backfill soil.

1 INTRODUCTION

The seismic behavior of a retaining structure is a complex soil–structure interaction problem. The seismic wall response and dynamic earth pressures are affected by the response of the backfill, the inertial and flexural responses of the wall itself and the input earthquake motions. In engineering practice, the seismic design of retaining structures is conventionally carried out using the pseudo-static approach, where dynamic actions are considered as static D'Alembert forces proportional to an equivalent acceleration. The Mononobe–Okabe (MO) method (Mononobe & Matsuo 1929, Okabe 1926) uses Coulomb's earth pressure theory and was originally developed for gravity walls retaining cohesionless backfill materials.

The MO method and/or its modification by Seed & Whitman (1970) are widely used in practice; they are generally used as a standard for the seismic design of gravity- and cantilever-type retaining walls. In MO theory, retaining walls move during earthquakes under the hypothetical conditions of Coulomb's theory, which assumes that the backfill is in a state of plastic equilibrium. The dynamic earth pressure can be obtained by applying a uniform acceleration to a specific failure wedge of the backfill. Although uncertainty remains regarding the position of the dynamic earth pressure and height effects of the site amplification, several experimental studies have agreed that the MO method gives appropriate results for seismic design (Seed & Whitman 1970, Ortiz 1982, Steedman & Zeng 1990). The latest NCHRP report (Anderson et al. 2009) recommended the use of the MO method for the seismic design of cantilever walls. The current AASHTO LRFD bridge design specifications suggest that a seismic coefficient equal to half the peak ground acceleration be used in the design and ignore the inertial forces of the wall. Most recently, Nakamura (2006) and Atik & Sitar (2010) performed dynamic centrifuge experiments on gravity- and cantilever-type retaining walls, respectively. They concluded that the MO method does not reflect either the actual seismic behavior of the wall–backfill interaction or the inertial effect of the wall itself. Even though the MO method provides a simple and powerful tool for evaluating the dynamic earth pressure, the assumptions of the MO method show an apparent discrepancy between the analysis and real behavior. Furthermore, MO theory does not consider the inertial force and effect of wall height.

In the present study, two dynamic centrifuge experiments were performed to simulate inverted T-shape retaining walls and reexamine the previous research. The obtained results were compared to the hypothetical conditions of MO theory. To investigate the effects of the wall height and inertial force, two different retaining wall heights were selected; the heights were represented as 5.4 and 10.8 m at the prototype scale.

2 EXPERIMENTAL PROCEDURE

Two dynamic centrifuge tests were performed with inverted T-shape retaining wall models. The experiments were conducted using the dynamic centrifuge at the KOCED Geo-Centrifuge Test Center at KAIST (Fig. 1). The maximum capacity of the KAIST centrifuge with a 5 m radius is 2400 kg for

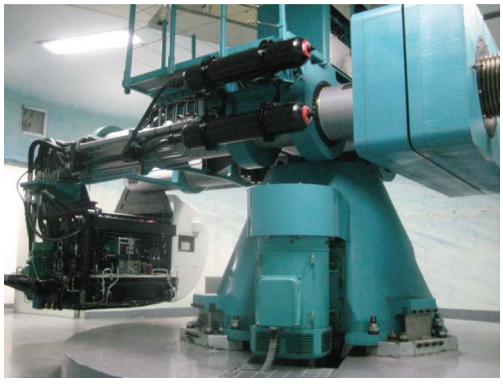

Figure 1. KAIST geo-centrifuge with earthquake simulator.

a centrifugal acceleration of up to 100 g. Details on the technical specifications for the centrifuge are available in the literature (Kim et al. 2013a). An earthquake loading was simulated by an in-flight earthquake simulator equipped with an electro-hydraulic system. It can generate random earthquake excitations lasting up to 1 s with model frequencies of 30–300 Hz (Kim et al. 2013b).

In this study, the models were constructed in an equivalent shear beam box (Lee et al. 2013) and a centrifugal acceleration of 50 g was used in the two experiments. All results are presented in terms of prototype units of measurement unless otherwise stated.

2.1 *Model structures and instrumentation*

The inverted T-shape retaining wall models used in the experiments were made of aluminum alloy (Fig. 3). At the prototype scale, the heights of the retaining walls were 5.4 and 10.8 m. The corresponding thicknesses of the walls were 0.22 and 0.35 m. The models were designed to be very flexible compared with ordinary cantilever and gravity retaining walls, which are stiff. The wall thickness was selected using the minimum value that can resist dynamic earth pressure as calculated by MO theory. Ortiz (1982) used the equilibrium method between the dynamic earth pressure and allowable strength of the wall based on the material property of the tensile yield strength. The test setup is shown in Figure 2. At the prototype scale, the estimated natural periods of the walls were 0.23 and 0.55 s, respectively. Both structures spanned the width of the container (Fig. 4). The scale law of the mass was not considered. Although the inertial force is affected by the mass of the wall, the experiments were focused on comparison with the hypothetical conditions of MO theory and investigating the

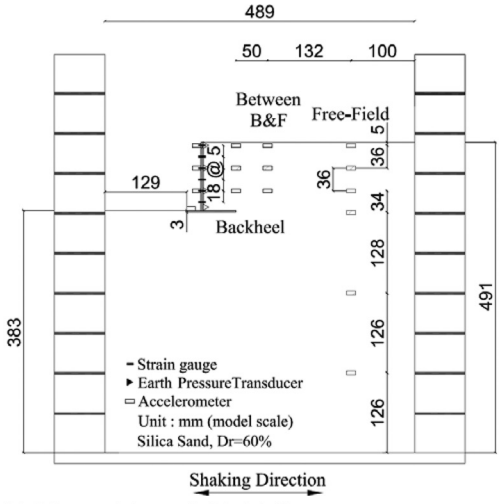

(a) 5.4 m retaining wall (Model A).

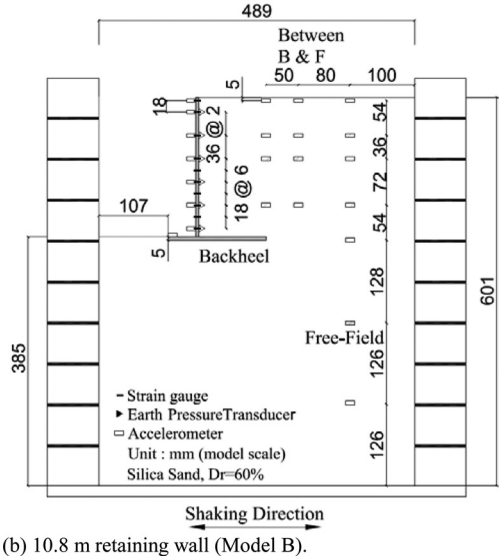

(b) 10.8 m retaining wall (Model B).

Figure 2. Model preparation and monitoring locations.

effects of the wall height and inertial force. Sandpaper was attached to the bottom of the wall base to increase the friction angle between the soil and wall base.

The accelerometers were placed at various heights and locations, as shown in Figure 2. Locations in the model were named "wall", "backheel", "between backheel and free field" and "free field" as shown in Figure 2a. The earth pressures were measured by miniature transducers attached to the wall and back-calculated based on bending moments measured by strain gauges on the wall. The acceleration and bend-

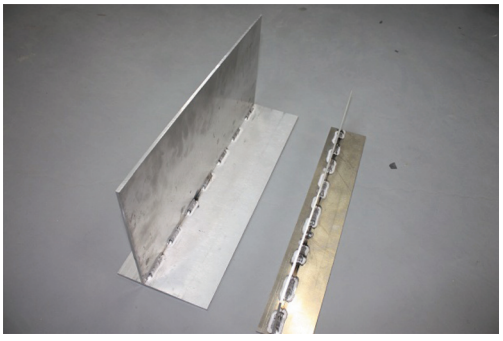

Figure 3. Retaining wall models for the test (inverted T-shape).

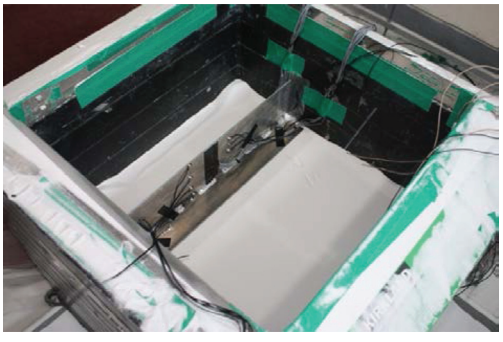

Figure 4. Installation of retaining wall during preparation.

ing moment were positive in the active directions (outwards from the backfill). The horizontal displacements were estimated by double integration of the acceleration.

2.2 *Test model preparation*

This experiment used silica sand produced by the hammer crusher process. The soil was prepared by dry pluviation.

The relative density was about 60% ($\gamma_d = 1.45$ t/m^3). The same soil densities were produced by calibrating the drop height, opening and speed of the pluviator. The internal friction angle was about 41° in a triaxial test. The shear wave velocity was measured using block bender elements at the same depths with two accelerometers in the sand underneath the structure. The average shear-wave velocity was about 170 m/s. The estimated natural period of the base soil prior to shaking was 0.48 s.

The sequence of model construction is as follows. (1) A 380 mm thick sand layer was prepared underneath the structures by pluviation. (2) The retaining wall was placed at its designed location (Fig. 4). (3) Sand was pluviated up to the surface height again. (4) Afterward, the front soil of the wall was removed by a vacuum cleaner. (5) Finally, the surface was smoothed with the vacuum cleaner. All instruments were placed at their pre-designed locations during pluviation. Industrial grease was placed between the model wall and the side walls of the container to reduce friction at the wall–container boundaries. Plastic sheets were attached to prevent sand from passing through those boundaries.

Table 1. Input motions PGA.

	Model A, 5.4 m	Model B, 10.8 m
Earthquake	Units: g	Units: g
Ofunato	0.04	0.06
	0.13	0.15
	0.26	0.27
	0.36	0.39
Hachinohe	0.05	0.05
	0.18	0.19
	0.27	0.27
	0.36	0.37

2.3 *Earthquake input motions*

Two types of input motions were used to simulate earthquakes: Ofunato and Hachinohe. The Ofunato record is characterized by a short period dominant earthquake, which is most likely to occur in Korea. In contrast, the Hachinohe record is a long period dominant earthquake and was used to compare the behavior from the Ofunato record. The earthquake was orthogonally applied to the retaining wall model. Stage tests were conducted for each model. The peak accelerations of the bedrock motion were 0.04–0.35 g. The amplitude, frequency and duration of input motions were scaled for the centrifuge test. Table 1 lists the input accelerations used for the stage tests.

3 TEST RESULTS AND DISCUSSIONS

3.1 *Phase difference*

To compare the behaviors in the free field, backfill soil and retaining wall effectively, as shown in Figure 5, which shows the acceleration–time histories at different depths (i.e. 2.35 and 8.35 m from the surface) in the 10.8 m wall (Model B) with the Ofunato earthquake. Near the wall base, the acceleration of the wall was almost synchronous with the accelerations of the backfill soil and free-field

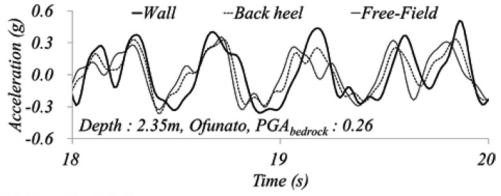

(a) Depth: 2.35 m.

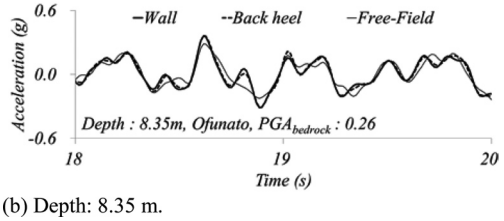

(b) Depth: 8.35 m.

Figure 5. Phase difference with depth (model B).

motions (Fig. 5b). However, a certain phase difference existed in time signals between the wall and backfill soil at shallow depths (Fig. 5a). The retaining wall showed the highest acceleration amplitude and the largest phase difference occurred with free-field motion.

MO theory assumes that no phase difference occurs between the motions of the retaining wall and backfill. In reality, differences in phase and amplitude occurred. Therefore, in contrast to MO theory, the acceleration of the soil wedge behind the wall is not uniform.

3.2 *Acceleration measurements with heights*

Figure 6 shows the variations in peak accelerations with depth at the 5.4 m and 10.8 m retaining walls (Models A and B, respectively) under Ofunato loadings from low to high magnitudes. As shown in the figure, the peak acceleration in the free field increased consistently from the bedrock to the surface under weak earthquake motion, whereas the peak acceleration was dampened up to the depth of the base owing to the nonlinear characteristics of the soil subjected to a strong earthquake.

The amplification trends are clearly shown by the normalized amplification ratios on the ground surface in Figure 7. In both models, accelerations in the free field were amplified the least and accelerations at the retaining walls were amplified the most. The average amplification ratios at the backheel and free field were around 2.0 for both Models A and B under the Ofunato loading. Amplification ratios of Model A under the Hachinohe loading were less than 1.5. The average amplification ratios of the backheel and wall were 2.5 except for the Model A under the Hachinohe loading.

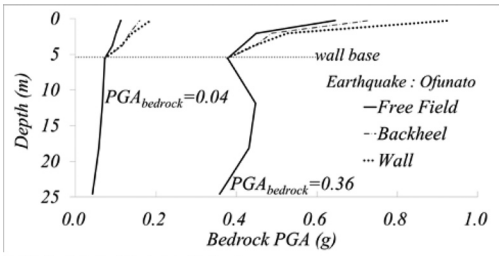

(a) Model A (Height: 5.4 m).

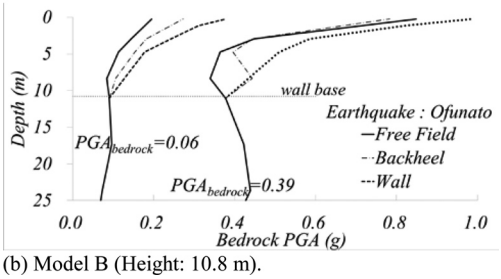

(b) Model B (Height: 10.8 m).

Figure 6. Acceleration characteristics under Ofunato earthquake.

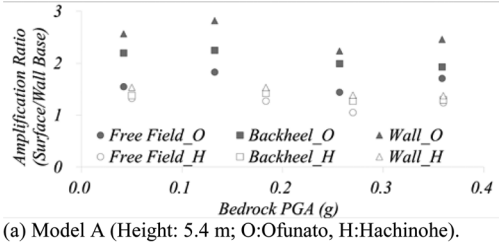

(a) Model A (Height: 5.4 m; O:Ofunato, H:Hachinohe).

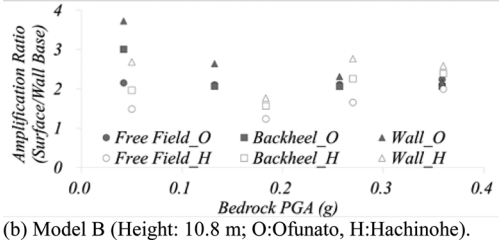

(b) Model B (Height: 10.8 m; O:Ofunato, H:Hachinohe).

Figure 7. Amplification ratio from wall base to surface.

In particular, the amplification ratio of Model B for the free field, backheel and wall converged to 2.0–2.5. The amplification ratio was also affected by the earthquake loading characteristics.

The NCHRP report (Anderson et al. 2009) suggests a "height dependent reduction scaling factor" of the seismic coefficient for seismic design. In the present study, however, the amplification ratios of the backheel and retaining wall were similar in

both Models A and B even though the wall height was increased twice. Contrary to general expectation (i.e. amplification increases with the wall height) the amplification ratios for the backfill soil and wall were not affected by the wall height. The amplification ratio at the free field in Model B was higher than that in Model A; this phenomenon may be caused by the different soil depths for the two models.

As shown in Figure 7, the earthquake had a clear effect on the amplification ratio in Model A, but the difference between the Ofunato and Hachinohe earthquake results decreased in Model B. The natural frequencies of the walls in Models A and B were 4.35 and 1.81 Hz, respectively. The natural frequencies of the backfill layer above the wall base were 7.87 and 3.93 Hz in Models A and B, respectively. The Ofunato earthquake contained high frequencies (i.e. 2–6 Hz).

In Model A, the backfill soil was super-resonant, but the retaining wall was resonant. Therefore, the amplification ratio of the wall in Model A was much higher when subjected to the Ofunato earthquake than to the Hachinohe earthquake; this induced the large difference in amplification ratio between the wall and free field. The natural frequency of the wall was much lower in Model B than in Model A. Therefore, the high frequency had a reduced effect. The Hachinohe earthquake contained low frequencies (i.e. 1–2 Hz) and the retaining wall was resonant in this range. Thus, the difference in amplification ratio between the wall and free field was larger for the Hachinohe earthquake than for the Ofunato earthquake.

MO theory assumes that the retaining wall and the soil wedge behave as rigid bodies and that a uniform acceleration is applied to the failure wedge behind the wall in the estimation of dynamic earth pressures. However, according to the test results, acceleration was amplified along the depth within the soil wedge of the backfill above the wall base. Thus, the retaining wall and soil wedge cannot be considered as rigid bodies, contrary to MO theory.

3.3 *Seismic earth pressure on the wall*

Lateral earth pressures were measured directly along the entire height of the wall using soil pressure transducers.

Nakamura (2006) showed that earth pressures change over time and that the pressure distribution changes with types of base shaking. Atik & Sitar (2010) reported that the maximum total earth pressure and bending moment profiles correspond to when the maximum moment is recorded at the lowest strain gauge on the walls and that the maximum earth pressure profiles monotonically increase with depth. However, in this study, earth pressures measured at different depths were not in phase. The earth pressure measured at the deepest depth had a phase opposite to those measured at shallow depths owing to deflection of the wall induced by the inertial force of the wall (Fig. 8).

Figure 9 shows the relation between the moment and earth pressure at the lowest strain gauge and pressure transducer. When the moment was a local maximum, which is the most critical situation for structural safety, the dynamic earth pressure was not a local maximum and actually almost zero in Model B. The phase difference between the moment and earth pressure was particularly distinct in Model B. These results indicate that bending moments of flexible walls are influenced by inertial effects as well as dynamic earth pressures.

MO theory does not consider the phase difference between a wall and backfill soil during an earthquake. MO theory considers the inertial force of the entire soil wedge behind the wall as an equivalent static force acting on the rigid wall. However, the flexible retaining wall was not rigid

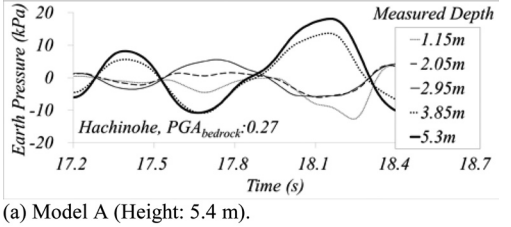

(a) Model A (Height: 5.4 m).

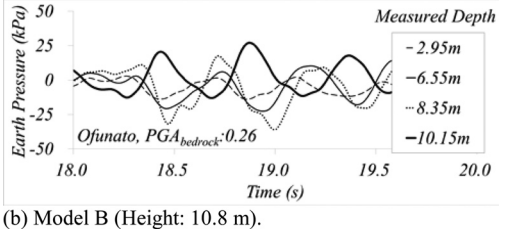

(b) Model B (Height: 10.8 m).

Figure 8. Phase difference in earth pressure with depth.

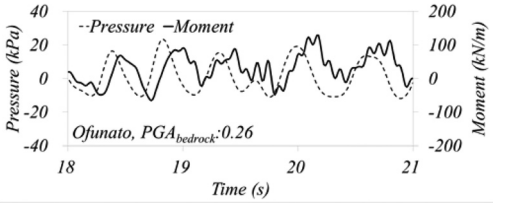

Figure 9. Phase difference between moment and dynamic earth pressure (model B).

enough and the behavior of the wall was affected by the inertial force of the wall itself along its height.

Figure 10 shows the dynamic moment, dynamic earth pressure and displacement when the maximum moment was recorded at the deepest strain gauge of the walls during an earthquake. Bending moments were at a maximum; however, dynamic earth pressure only appeared at the bottom area of the wall. Negative dynamic earth pressures imply a loss of contact between the wall and backfill soil. Displacements of the wall and soil were calculated by double integration of the acceleration obtained on the wall along the height. The active direction represents the positive displacement. The top of the wall contained gaps between the wall and backfill during the earthquake. Although the moment was at a maximum and the wall deflected, the dynamic earth pressure was less than the earth pressure of the static state except along deeper parts of the wall. The gap between the wall and backfill soil was larger for the 10.8 m wall than for the 5.4 m wall.

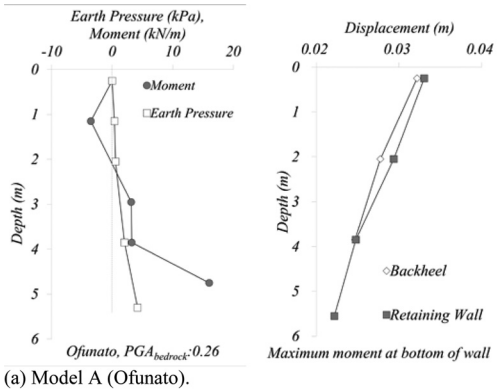

(a) Model A (Ofunato).

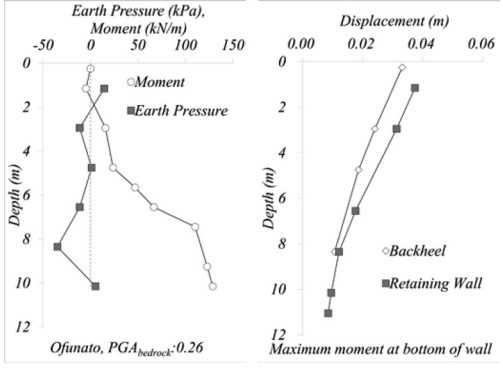

(b) Model B (Ofunato).

Figure 10. Dynamic bending moments, earth pressure and displacement when maximum moment was recorded at the deepest strain gauge.

These results illustrate that not only the dynamic earth pressure but also the inertial force of the wall itself affects the bending moment of the wall. The bottom of the wall was fixed to the wall base and its deflection was restricted by the wall base; in contrast, the upper part of the wall was relatively free to deform. In this study, the flexible wall easily deformed and the backfill soil could not catch up with the wall displacement during earthquakes. At this moment, a gap was generated and the earth pressure was not in phase with the bending moment. This phenomenon suggests that the inertial force of a flexible cantilever wall is an important factor that affects bending moments during earthquakes. In contrast with MO theory, the inertial effects of the wall have to be evaluated for cantilever-type retaining walls subjected to seismic loads.

4 CONCLUSIONS

This study aimed to simulate two inverted T-shape cantilever retaining walls with different heights under a scaling ratio of 50 using a dynamic centrifuge to qualitatively present their seismic behavior. These two retaining walls had different heights and stiffness. However, their stiffness were flexible and the models were subjected to input motions from Ofunato and Hachinohe earthquakes. The accelerations of the backfill area were amplified up to around 2.0–2.5. For Model B (height: 10.8 m), the amplification ratio was similar to Model A (height: 5.4 m) and converged to 2.0. Moreover, the dynamic earth pressure when the maximum moment was recorded at the lowest strain gauge of the walls during the earthquake was not synchronized and almost zero. The inertial force of the wall-induced deflection of the wall resulted in a gap between the wall and backfill soil. The results of this study can offer basic understanding about the seismic behavior of flexible inverted T-shape retaining walls. Further experiments with comparatively stiff and rigid walls and numerical analysis are currently underway to verify the behavior of flexible retaining walls.

ACKNOWLEDGMENTS

The experiments were carried out in the KOCED Geo-Centrifuge Facility using KREONET. This research was supported by a grant (11 Technology Innovation D02) from the Construction Technology Innovation Program funded by the Ministry of Land, Infrastructure and Transport of the Korean government.

REFERENCES

Anderson, D.G., Martin, G.R., Lam, I. & Wang, J.N. 2009. *Seismic Analysis and Design of Retaining Walls, Buried Structures, Slopes, and Embankments*. Washington, D.C.: Transportation Research Board.

Atik, L.A. & Sitar, N. 2010. Seismic earth pressures on cantilever retaining structures. *Journal of Geotechnical and Geoenvironmental Engineering* 136(10): 1324–1333.

Kim, D.S., Kim, N.R., Choo, Y.W. & Cho, G.C. 2013a. A newly developed state-of-the-art geotechnical centrifuge in Korea. *KSCE Journal of Civil Engineering* 17(1): 77–84.

Kim, D.S., Lee, S.H., Choo, Y.W. & Rames, D. 2013b. Self-balanced earthquake simulator on centrifuge and dynamic performance verification. *KSCE Journal of Civil Engineering* 17(4): 651–661.

Lee, S.H., Choo, Y.W. & Kim, D.S. 2013. Performance of an equivalent shear beam (ESB) model container for dynamic geotechnical centrifuge tests. *Soil Dynamics and Earthquake Engineering* 44: 102–114.

Mononobe, N. & Matsuo, H. 1929. On the determination of earth pressures during earthquakes. *World Engineering Congress*: 179–187.

Nakamura, S. 2006. Re-examination of Mononobe-Okabe theory of gravity retaining walls using centrifuge model tests. *Soils and Foundations* 46(2): 135–146.

Okabe, S. 1926. General theory of earth pressures. *Journal of the Japanes Sociey of Civil Engineers* 12(1): 123–134.

Ortiz, L.A. 1982. *Dynamic Centrifuge Testing of Cantilever Retaining Walls*. Ph.D. thesis, California Institute of Technology.

Seed, H.B. & Whitman, R.V. 1970. Design of earth retaining structures for dynamic loads. Proc., Specialty Conference on Lateral Stresses in the Ground and Design of Earth Retaining Structures, Cornell Univ. Ithaca, 22–24 June 1970. New York: ASCE.

Steedman, R.S. & Zeng, X. 1990. The influence of phase on the calculation of pseudo-static earth pressure on a retaining wall. *Géotechnique,* 40(1): 103–112.